HHS Public Access

Author manuscript

Nat Immunol. Author manuscript; available in PMC 2011 March 08.

Published in final edited form as:

Nat Immunol. 2010 August ; 11(8): 743–750. doi:10.1038/ni.1897.

The transcription factor MAFB antagonizes anti-viral responses by blockade of coactivator recruitment to IRF3

Hwijin Kim and **Brian Seed***

Center for Computational and Integrative Biology, Massachusetts General Hospital, Boston MA 02114, USA, Department of Genetics, Harvard Medical School, Boston MA 02115, USA, Phone: 617-726-5975. Fax: 617-643-3328

Brian Seed: bseed@ccib.mgh.harvard.edu

Abstract

Viral infections induce Type I interferons (IFN-α and -β) that recruit unexposed cells in a self-amplifying response. We report that the transcription factor MAFB thwarts auto-amplification by a metastable switch behavior. MAFB acts as a weak positive basal regulator of transcription at the *IFN-β* promoter through activity at AP-1-like sites. Interferon elicitors recruit the transcription factor IRF3 to the promoter, whereupon MAFB acts as a transcriptional antagonist, impairing the interaction of CREB-binding protein (CBP) with IRF3. Mathematical modeling supports the view that prepositioning of MAFB on the promoter allows the system to respond rapidly to fluctuations in IRF3 activity. Elevated expression of MAFB in human pancreatic islet β-cells might increase cellular vulnerability to viral infections associated with the etiology of type I diabetes.

Keywords

MAFB; interferon; diabetes; antiviral; model

Viral infections in mammalian cells elicit responses by strain-nonspecific cellular pattern-recognition receptors, including Toll-like receptors (TLRs), RIG-like helicase, double-strand-specific kinases, and cytosolic DNA receptors[1]. Engagement of these sensors triggers an intracellular signaling cascade leading to the production of type-I interferon (IFN-I) and proinflammatory cytokines. The cytokines further activate a subset of genes that enforce and propagate an antiviral state throughout the host, thereby activating the first line of defense against viral pathogens. Although rapid and sensitive cellular induction of cytokines upon virus infection is essential for efficient suppression of viral propagation, mammalian cells have also developed multiple mechanisms to prevent autonomous induction and excess production of Type I IFNs[2]. Despite major advances over the last decade in our

*Corresponding Author: Mailing Address: CPZN 7-7228, Massachusetts General Hospital, 185 Cambridge Street, Boston, MA 02114. Phone: 617-726-5975. Fax: 617-643-3328. bseed@ccib.mgh.harvard.edu.

Author Contributions

H.K. designed and performed experiments and wrote the manuscript; B.S. designed and supervised research and wrote the manuscript.

understanding of cellular regulation of Type I IFN induction and signaling pathways, the components of the pathways involved have not been fully elucidated.

In this study, a genome-wide screen of potential gene products interacting with the human type I interferon transcriptional response identified multiple candidates with negative action at the interferon β promoter. One of these, *MAFB*, a member of the family of MAF transcription factors, is the subject of this report. Members of the MAF family of proto-oncogenes mediate both oncogenic transformation and terminal differentiation[3,4]. *MAFB* is ubiquitously expressed in human tissues[5], but is found at an especially high amounts in myeloid cells, and facilitates the establishment and maintenance of the monocyte-macrophage lineage[6]. *MAFB* has also been implicated in the formation of pancreatic islet beta cells[7,8]. We report here that *MAFB* is a regulator of Type I IFN transcription with a dual mode of action as both activator and coactivation inhibitor.

Results

MAFB is a negative regulator of Type I IFN

Candidate positive and negative regulators of Type I IFN transcription were identified by a transcriptional reporter screen in which 17184 individual cDNAs encoding human proteins were cotransfected with an *IFN-β* luciferase reporter into 293ETN cells. Luciferase activity measured at 2 days post-transfection provided a sensitive and reliable measure of transcriptional enhancement or repression. The screen identified known activators and repressors of *IFN-β* transcription as well as proteins for which no activity had previously been ascribed. Among the latter, the large MAF family protein *MAFB* consistently and prominently inhibited the interferon transcriptional response and was selected for further study.

Overexpression of *MAFB* in 293ETN cells weakly enhanced the basal activity of the *IFN-β* promoter in a dose-dependent manner (Fig. 1a). By contrast, when the cells were primed with poly(I:C) at 24 h post-transfection, coexpressed *MAFB* strongly inhibited activation (Fig. 1a). *MAFB*-mediated inhibition did not reflect a general repression of transcription since the activity of a luciferase expressed under the control of a *Herpes simplex* thymidine kinase promoter was not affected by *MAFB* coexpression either in the absence or presence of poly(I:C) (Fig. 1b). In addition, the activities of p53-and NF-κB-promoter luciferase reporters were not suppressed by coexpressed *MAFB* (Fig. 1b). *MAFB* strongly inhibited *IFN-β* activation triggered by other *IFN-β* inducers, including constitutively active N-terminal forms of *RIG-I* and *MDA5*[9,10], *RIG-I(N)* and *MDA5(N)*, respectively, and Newcastle disease virus (NDV) (Fig. 1c). Similar results were obtained using HEC1B cells (Supplementary Fig. 1a), which lack a functional type I IFN receptor, indicating that suppression of extracellular feedback mediated by *IFN-β* secretion is not a required element of the inhibition process. *Mafb* also inhibited poly(I:C)- and *RIG-I(N)*-mediated activation of *Ifn-β* in murine macrophage cell lines (Supplementary Fig. 1b). The action of *MAFB* on endogenous *IFN-α* and *β* promoters recapitulated the results found with the synthetic promoter. In unstimulated 293ETN cells the basal expression of *IFN-β* and *α1* mRNAs was slightly increased by *MAFB* overexpression, whereas the poly(I:C)-mediated activation was severely impaired (Fig. 1d and e). The luciferase activity of a recombinant vesicular

stomatitis virus (VSV-Luc) was enhanced by coexpression of *MAFB*, whereas expression of *IRF3*, a positive regulator of Type I IFN induction, suppressed VSV-dependent luciferase expression (Fig. 1f).

To clarify which DNA motif within the *IFN-β* promoter conveyed the observed *MAFB* effects, we cotransfected *MAFB* expression plasmids with luciferase reporters containing multimerized PRDIII-PRDI (P31CS), PRDIV (AP-1) or PRDII (NF-κB) motifs, which bind *IRF3* and *7*, *ATF2* and *c-JUN*, and *NF-κB* (*p50* and *p65*) transcription factors, respectively[11]. In unstimulated cells, the AP1 motif was activated by *MAFB* coexpression (Fig. 1g), suggesting that this motif is responsible for *MAFB*-mediated stimulation of *IFN-β* promoter basal activity. Upon poly(I:C) treatment, the P31CS motif was strongly activated (> 50-fold), and this activation was potently inhibited by *MAFB* coexpression (Fig. 1g). Coexpression of *MAFB* with a reporter based on the *ISG54* ISRE element (regulated by *IRF3* and *7*) corroborated these findings (Supplementary Fig. 1c). Mutation of the PRDIII-PRDI motif of the *IFN-β* promoter that diminishes binding of *IRF3* and *7*[12] led to decreased *MAFB*-mediated inhibition of poly(I:C) induction (Fig. 1h). *MAFB* had little inhibitory effect on the activation by *IFN-β* inducers or *MyD88* of NF-κB motif-dependent transcription, as exemplified by a mutant *IFN-β* reporter containing the PRDII motif but lacking PRDIII-PRDI and PRDIV (Fig. 1h) or by multimerized NF-κB (Supplementary Fig. 1d). In addition, *MAFB* did not inhibit activation of the intact *IFN-β* promoter by TNF and phorbol myristate acetate (PMA), which act via NF-κB and AP-1 motifs, respectively, and the PRDIII-PRDI mutant *IFN-β* promoter by *MyD88* (Fig. 1h). These results argue against the possibility of nonspecific suppression of *IFN-β* activation by *MAFB* coexpression. The *RANTES* (*CCL5*) promoter was similarly regulated by *MAFB* in a signal-dependent manner (Supplementary Fig. 1c), indicating that the regulatory activity of *MAFB* is not restricted to the *IFN-β* promoter. The apparent action of *MAFB* at AP-1 motifs is consistent with the observation that the canonical MAF response element, MARE, contains an AP1 motif as its core (Supplementary Fig. 1c)[3],[4]. Collectively, these data support the view that the stimulatory and inhibitory activities of *MAFB* at the *IFN-β* promoter segregate with the AP-1 site and *IRF3* and *7* binding site respectively, and that the inhibitory action of *MAFB* at *IRF3* and *7* binding sites is not confined to the *IFN-β* promoter.

MAFB deficiency facilitates Type I IFN production

Although *Mafb* null homozygotes display a perinatal lethal phenotype, the innate antiviral responses of $Mafb^{-/-}$ mouse embryonic fibroblasts (MEFs) could be contrasted with those of MEFs generated from $Mafb^{+/-}$ heterozygous littermates[13]. In the basal state, *Ifn-α* and *β* mRNA abundance was significantly higher in homozygous MEFs compared to heterozygous control MEFs (Fig. 2a). Transcripts of genes induced by Type I IFN signaling, such as *Irf7* and *Rig-I*, were also more highly expressed in homozygous MEFs compared to heterozygous controls (Supplementary Fig. 2a). Poly(I:C) treatment elicited significantly higher quantities of *Ifn-α* and *β* mRNA (Fig. 2a) and secreted *Ifn-β* (Fig. 2b) in homozygous MEFs. Introduction of a plasmid encoding luciferase under the control of the mouse *Ifn-β* promoter revealed that activation by poly(I:C) treatment or NDV infection was greater in homozygous MEFs than in heterozygous MEFs (Fig. 2c). In addition, reintroduction of mouse *Mafb* in *Mafb* null MEFs attenuated *Ifn-β* activation by poly(I:C) or NDV (Fig. 2d).

In accord with the more robust antiviral responses observed in the knockout MEFs, VSV-Luc expression was diminished in homozygous MEFs compared to heterozygous MEFs (Fig. 2e).

Homozygous MEFs grew more slowly than heterozygous MEFs, suggesting that the chronic activation of Type I IFN genes might retard growth. Potential *MAFB* influences on apoptosis induced by viruses or virus-mimetic signals were assessed by measuring caspase 3 activity in homozygous and heterozygous cells (Supplementary Fig. 2b). No difference in caspase 3 activities was observed between null and heterozygous MEFs in the absence of a viral trigger. However, upon poly(I:C) treatment, caspase 3 activity significantly increased in homozygous, but not in heterozygous MEFs (Supplementary Fig. 2b).

The general features of *MAFB*-mediated regulation of IFN transcription in murine fibroblasts were also found in human cells of diverse origin. Short hairpin or small interfering RNAs targeting *Mafb* mRNA (Supplementary Fig. 2c) promoted activation of the human *IFN-β* promoter triggered by poly(I:C) treatment in 293ETN cells (Supplementary Fig. 2d), HeLa and HT-1080 cells (Supplementary Fig. 2e). Thus *MAFB* is a broadly expressed transcription factor that has an important function in the restraint of *IFN-β* promoter activity.

MAFB interferes with IRF3 activity

The downstream signaling machinery common to *RIG-I*, *MDA5* and *TLR3* includes the kinases *TBK1* and *IKKε*[14,15] and the transcription factors *IRF3* and *IRF7*[16,17]. Coexpression of *MAFB* strongly repressed Type I IFN induction mediated by the upstream effectors of *IRF3* and *IRF7*, as well as *IRF3* and *IRF7* themselves, in 293ETN cells (Fig. 3a). Similar results were obtained when cells were stimulated using poly(I:C) (Supplementary Fig. 3a). *MAFB* repressed the *IFN-β* activation mediated by a constitutively active form of *IRF3*, *IRF3(5D)*[18,19] (Supplementary Fig. 3a), supporting the interpretation that *MAFB* functions at a step downstream of *IRF3* C-terminal phosphorylation by *TBK1* or *IKKε*. Following transfection, *MAFB* was found exclusively in the nucleus by immunohistochemistry (Supplementary Fig. 3b) and immunoblotting (Supplementary Fig. 3c), and this localization was unaffected by virus infection, suggesting that the action of *MAFB* is likely intranuclear.

In untransfected HeLa cells, a weak basal association of endogenous *MAFB* with *IRF3* was found to increase considerably after poly(I:C) stimulation without elevation of *MAFB* and *IRF3* abundance (Fig. 3b). Similar results were obtained using HepG2 cell extracts (Supplementary Fig. 4a), suggesting that the association is not cell type-specific. To evaluate the possibility that *MAFB* interacts with *IRF7*, 293ETN cells were transfected with hemagglutinin (HA)-tagged *MAFB* together with Flag-tagged *IRF7*. As a specificity control, the interaction of HA-*MAFB* and Flag-tagged *TBK1* was also examined. *MAFB* associated with *IRF7*, but not with *TBK1*, in unstimulated cells (Fig. 3c). Upon poly(I:C) stimulation (Supplementary Fig. 4b), the interaction between *MAFB* and *IRF7* appeared to grow stronger, whereas *MAFB* remained unassociated with *TBK1*.

Because *MAFB* effectively suppresses *IFN-β* promoter activation by a range of stimuli in HEC1B cells (Supplementary Fig. 1a), in which the inhibitory effect of *MAFB* is likely

mediated through *IRF3*[20], we explored potential interactions between *IRF3* and *MAFB* using a series of Flag-tagged *IRF3* deletion mutants (Fig. 3d) and HA-tagged *MAFB* (Supplementary Fig. 4c). Full length *MAFB* coimmunopreciptated with full length *IRF3* and deletion mutants containing the C-terminal IRF association domain (IAD), N3(1-394), C1(134-427) and C2(197-427) fragments, but not with the N-terminal portion of *IRF3*, N1(1-134) and N2(1-197) (Fig. 3d). This demonstrated that the interaction between *MAFB* and *IRF3* requires the intact IAD of *IRF3*, whereas the N-terminal DNA binding domain of *IRF3* is dispensable for the *MAFB–IRF3* interaction. All *MAFB* deletion mutants could be detected following coimmunoprecipitation with *IRF3* (Supplementary Fig. 4c). However, substantial disparities in amounts of *MAFB* protein expression were present, and an expression-normalized assessment suggests that the C-terminal basic leucine zipper (bZIP) domain of *MAFB* contributes strongly to the association with *IRF3*, possibly by facilitation of dimerization. *MAFB* also exerted inhibitory influences on *IRF7*-dependent (but *IRF3*-independent) transcriptional activation (Supplementary Fig. 5a). Efficient binding of *MAFB* to *IRF7* requires the N-terminal portion of *IRF7* including the DNA binding domain (Supplementary Fig. 5b).

IRF3 is localized predominantly in the cytoplasm in uninfected cells. Upon virus infection, *IRF3* is activated through phosphorylation at its C-terminal serine residues, relieving an intramolecular autoinhibitory association. This conformational change leads to formation of homodimers, accumulation in the nucleus, stimulation of DNA binding, and association with the CBP or p300 coactivator, and thereby activating the Type I IFN genes[19–22]. Poly(I:C) stimulation substantially increased the formation of heterodimers between Flag-*IRF3* and HA-*IRF3*, but *MAFB* coexpression only weakly suppressed *IRF3* dimer formation (Supplementary Fig. 6a). Similar results were obtained when *IRF3* dimerization was analyzed using native PAGE in the presence of deoxycholate[20] (Supplementary Fig. 6b).

To study the effect of *MAFB* on *IRF3* DNA binding, we carried out electrophoretic mobility shift assays (EMSAs) using a PRDIII-PRDI (P31) oligonucleotide from the *IFN-β* promoter or an ISRE element from the *ISG15* promoter as a probe (Fig. 4a). Addition of *in vitro* translated His-*MAFB* did not have an observable effect on the binding of immunopurified *IRF3*-Flag to the P31 or ISG15 motif (Fig. 4a, lanes 4–6 and 10–12). Similarly, addition of 293ETN-expressed and immunopurified Flag-*MAFB* did not have any effect on the *IRF3* binding (Supplementary Fig. 6c). Equivalent results were obtained using nuclear extracts (NE) prepared from HEC1B cells (Supplementary Fig. 6d), which were transfected with C-terminal Flag-*IRF3(5D)* in the absence and in the presence of untagged *MAFB*. Binding of *MAFB* to the P31 motif could not be detected, although a weak binding of *MAFB* to the PRDIV motif was detected (Supplementary Fig. 6e).

The effect of *MAFB* on recruitment of *IRF3* to the *IFN-β* promoter *in vivo* was explored by chromatin immunoprecipitation (ChIP), followed by qPCR. Enrichment of *IFN-β* promoter sequences was detected in immunoprecipitates of endogenous *IRF3* from HeLa cells (Fig. 4b) or transfected 293ETN cells (Fig. 4c) and the enrichment was significantly enhanced by poly(I:C) stimulation. *MAFB* coexpression had either limited or no inhibitory effect on *IFN-β* promoter enrichment by activated *IRF3* (Fig. 4c). These results were confirmed by experiments relying on coexpression of *IRF3(5D)* and its Flag-tagged form (Fig. 4c). In

addition, we examined whether *MAFB* could be directly recruited to the *IFN-β* promoter. Immunoprecipitation of endogenous *MAFB* produced a robust enrichment of *IFN-β* promoter sequences from chromatin prepared from unstimulated HeLa cells, but upon poly(I:C) stimulation the enrichment diminished (Fig. 4b). Similar results were observed for transfected 293ETN cells expressing Flag-*MAFB* (Fig. 4d): promoter binding was compromised by *IRF3* coexpression and particularly by coexpression of constitutively activated forms of *IRF3*. Taken together, these results indicate that *MAFB* does not significantly interfere with DNA binding of *IRF3*. Instead, *IRF3* appears to displace *MAFB* upon activation and hence the action of *MAFB* must lie subsequent to *IRF3* binding. The transcriptional activation of Gal4-*IRF3* fusion proteins is suppressed by coexpressed *MAFB* thus supporting this notion (Fig. 4e). In addition, a DNA binding-defective mutant of *MAFB* (N248S)[23] retained inhibitory capacity at the *IFN-β* promoter (Supplementary Fig. 7a), although its transcriptional activity at MARE motifs was severely impaired (Supplementary Fig. 7b), suggesting that binding of *MAFB* to the *IFN-β* promoter is not a required element of the inhibition process[24]. Basal transcriptional activity of the Gal4-*IRF3*(1-394) truncation mutant (lacking the C-terminal activation domain) was somewhat higher than that of Gal4-*IRF3* (Fig. 4e), possibly attributable to a conformational change to an open structure[19–22]. No considerable increase in the transactivation by Gal4-*IRF3*(1-394) was observed upon poly(I:C) stimulation (Fig. 4e), and *MAFB* had little effect on transactivation by Gal4-*IRF3*(1-394), suggesting that *MAFB* interferes with functions of *IRF3* mediated through the C-terminal five Ser-Thr residues.

Because this region of *IRF3* can facilitate the recruitment and activation of the *CBP* or *p300* coactivator[19–22], we explored the possibility that *MAFB* directly interferes with *IRF3-CBP* interactions. A strong association was observed between Flag-*IRF3(5D)* and *CBP* (Fig. 4f, lane 5), and between Flag-*IRF3* and *CBP* upon poly(I:C) stimulation (Fig. 4f, lane 2). The introduction of *MAFB* or its Flag-tagged form severely impaired the association of *CBP* with activated forms of *IRF3* (Fig. 4f, lanes 3, 4 and 6). The relative strengths of *IRF3-CBP* interactions (Fig. 4f and Supplementary Fig. 7c) displayed a good correlation with the transactivation induced by Gal4-*IRF3* fusion proteins (Fig. 4e). Collectively, these results support the view that interference with *IRF3-CBP* interactions by *MAFB* is primarily responsible for the observed *MAFB*-mediated inhibition of *IRF3* and its Gal4 fusions (Fig. 3a and 4e and Supplementary Fig. 3a).

Ectopic expression of *CBP* did not lead to any observable reversal of the *MAFB*-mediated inhibition of *IRF3*-triggered *IFN-β* activation (Supplementary Fig. 7d). *MAFB* did not synergize with *CBP* at the *IFN-β* promoter (Supplementary Fig. 7e), and no interaction between overexpressed *CBP* and *MAFB* could be documented. *MAFB* also did not inhibit transactivation by the peroxisome proliferator-activated receptor gamma (*PPARγ*) and PPARγ coactivator-1α (*PGC1α*) (Supplementary Fig. 7f), which can synergize with *CBP* to activate transcription[25]. These results argue that *MAFB* does not compete with *IRF3* for binding to *CBP*, but rather competes with *CBP* for binding to *IRF3*.

We also examined whether sumoylation of *MAFB* was involved in inhibition of Type I IFN induction. All of the single and double sumoylation-deficient mutants of *MAFB* (K32R, K297R and K32,297R)[26] were as effective as wild-type *MAFB* in repressing poly(I:C)-

mediated activation of *IFN-β* (Supplementary Fig. 7g), indicating that the sumoylation status of *MAFB* is not linked with its ability to repress *IFN-β* activation. Taken together, the foregoing results indicate that *MAFB* acts as a transcriptional antagonist of Type I IFN induction primarily by impairing recruitment of the transcriptional coactivator *CBP* to *IRF3*.

Cellular regulation of MAFB expression

We next investigated how the expression of *MAFB* varies in response to a viral trigger. *MAFB* expression in 293ETN cells decreased upon poly(I:C) stimulation (Fig. 5a) and the expression of *MAFB* over time was inversely correlated with that of *IFN-α and β* (Fig. 1d and e). Expression of *c-MAF*, another member of the large MAF family protein, also declined in 293ETN cells (Fig. 5a) in response to poly(I:C) stimulation, and *c-MAF* suppressed *IFN-β* activation triggered by a range of Type I IFN inducers including poly(I:C), *RIG-I(N)* and *MDA5(N)* (Supplementary Fig. 8a). Expression of the large MAF transcription factors, *MAFA* and *NRL*, was modest compared to *MAFB* and *c-MAF* in 293ETN cells (data not shown). The change in *MAFB* abundance differs from that of other reported negative regulators of Type I IFN signaling pathway[2], such as *A20*, *DUBA* and *RNF125*, the expression of which is upregulated by viral triggers. Attenuation of *MAFB* expression upon induction suggests that *MAFB* acts principally to restrain Type I IFN production in response to low-level cues that might not reflect actual viral infections.

We also analyzed regulatory patterns of *MAFB* expression in a variety of cell types in response to pathogen-mimetic stimulation using publicly available microarray datasets including the GEO database (Fig. 5b–e, Supplementary Fig. 8b–e)[27–32]. In most cases, we observed that *MAFB* expression decreased in response to a pathogen-mimetic stimulus, whereas expression of *IFN-α* and *β* and genes regulated by *IFN-α* and *β* signaling increased. No systematic correlations could be detected for *c-MAF* and *NRL*, and in many cases their expression levels were negligible compared to that of *MAFB*. These results, combined with a broader tissue distribution of *MAFB* expression compared to other large MAF family members (http://biogps.gnf.org), suggest a general, lineage-nonspecific role for *MAFB*. However, some exceptions have been encountered. For example, in HeLa cells, *MAFB* expression increased slightly upon poly(I:C) stimulation, and induction of Type I IFN was much weaker than in 293ETN cells (Supplementary Fig. 8f). Expression of *MAFB* (Fig. 5f), and *c-MAF* (Supplementary Fig. 8g), was higher in an HCV-replicon-containing cell line that was selected to be highly permissive for HCV RNA replication[33]. The elevation in *MAFB* expression may be virus-dependent since inhibition of HCV replication by treating the cells with a cyclophilin inhibitor, Cyclosporin A (CsA), strongly reduced *MAFB* expression but had little effect on the uninfected parental line. These results raise the possibility that viruses induce *MAFB* as a strategy for suppressing Type I IFN responses.

Mathematical modeling of IFN-I induction

MAFB exhibits both stimulatory and inhibitory activities on the *IFN-β* promoter depending on experimental conditions (Fig. 1a). To provide a quantitative framework for understanding *MAFB*-mediated regulation of Type I IFN induction we developed a biochemical mass-action kinetic model, as outlined in the Supplementary Information. Using this model, we identified several key factors influencing the potency of *MAFB* as an inhibitor of the *IFN-β*

induction: high order interactions of *MAFB* and *IRF3* on the promoter and in the nucleoplasm, and a low order interaction of *MAFB* and *IFN-β* promoter, which affect the *IFN-β* promoter activity in opposing directions (Supplementary Fig. 9b–g and text therein). The model suggests that *MAFB*, even at a relatively low level, exerts a considerable inhibitory effect on *IFN-β* induction, primarily by a high order interaction of *MAFB* with *IRF3* on the promoter and resulting inhibition of *IRF3-CBP* pre-initiation complex formation (Supplementary Fig. 9e and f). These findings are in agreement with the experimental observations in genetically deficient MEFs. Rapid and strong induction of *IFN-β* in 293ETN cells in response to a viral elicitor can be ascribed to a substantially enhanced processing rate and higher efficiency of a pre-initiation complex for generating a productive Pol II elongation complex (Supplementary Fig. 9h and text therein). The complex between *MAFB* and *IRF3* in the nucleoplasm provides a mechanism to effectively buffer unwarranted low-level activation of *IFN-β*, and at the same time, combined with *MAFB* downregulation (Supplementary Fig. 9i), to counteract this buffering role of *MAFB* in order to facilitate the *IFN-β* activation upon virus infection (Supplementary Fig. 9j–n and text therein).

MAFB and enterovirus infection of pancreatic β cells

The finding that *MAFB* expression might predispose cells to viral infection suggests that cells highly expressing *MAFB* could be vulnerable to viruses. For example, *Enteroviruses* such as coxsackievirus are capable of infecting pancreatic tissues and such infection might be a trigger for the development of type I diabetes (T1D)[34,35]. Enterovirus infection is specific to endocrine pancreatic islet cells, but not to exocrine pancreas, in humans[35,36]. The known enterovirus tropism shows a good correlation with the pancreatic expression pattern of *MAFB* in humans (Fig. 6a)[37]. Further, *MAFB* expression is higher in purified human β cells (Fig. 6b)[38], which constitute over 60% of the islet population[32], than in islets themselves, suggesting that in humans *MAFB* expression is maintained at a relatively high level in mature β cells. By contrast, in mice, enterovirus infection of healthy islets is limited even in lethal cases[35,39], consistent with the relatively low level of *Mafb* expression in adult mouse islets[7]. *Mafb* expression is restricted to α cells in the adult mouse although the expression is observed both in α and β cells in the mouse embryo. To examine whether the differential *MAFB* expression might play a role in the observed cell tropism and species selectivity of enterovirus infection, human *MAFB* was ectopically expressed in a murine pancreatic β cell line, MIN6, and cellular antiviral responses were monitored. Coexpressed *MAFB* strongly inhibited activation of the murine *Ifn-β* promoter triggered by *RIG-I(N)* and *MDA5(N)* (Fig. 6c). In addition, *MAFB* expression considerably enhanced replication of VSV-Luc compared to a mock-transfected control (Fig. 6d). Because Type I interferon might play an essential role in preventing β cell destruction induced by coxsackievirus infection[40], it is possible that elevated *MAFB* expression in human islet cells might predispose these cells to coxsackievirus infection or persistence, thereby increasing susceptibility to type I diabetes. *Mafb* is a candidate gene within a T1D susceptibility locus, *Idd13*, in non-obese diabetic (NOD)/Lt mice[41].

Coxsackieviruses replicates in islet tissue of older prediabetic NOD mice[42]. To explore whether *Mafb* plays a role in age-dependent susceptibility of NOD mice to enterovirus

infection, we monitored *Mafb* expression in islet tissue. To avoid potential confounding effects of macrophage infiltration in islets, we selectively collected the β cell-rich core of islets using laser-capture microdissection (LCM). Elevated *Mafb* transcript abundance was detected in older NOD mice with severe hyperglycemia (blood glucose > 500 mg/dl) compared to younger NOD mice before the onset of hyperglycemia (Fig. 6e). The expression level of a macrophage-specific marker *Emr1* (encoding the F4/80) was below the limit of detection in all samples collected by LCM (data not shown). Similar results were obtained when whole islets were isolated from NOD mice by a conventional collagenase perfusion technique (Fig. 6f)[43], in which two age groups exhibited similar levels of macrophage infiltration. These results support the notion that the age-dependent accumulation of *Mafb* contributes to the observed susceptibility of older prediabetic NOD mice to enterovirus infection[42]. The extent to which endemic enteroviruses contribute to the etiology of NOD strain diabetes is presently unknown, but the variable course and age dependence are consistent with the influence of a stochastic environmental event. Species- and strain-specific, lineage-dependent *MAFB* expression can be predicted to contribute to susceptibility of islet β-cells to viral infection, a susceptibility that might contribute to the human susceptibility to type 1 diabetes.

Discussion

Results from studies on MEFs from *Mafb* deficient embryos in this work support the view that the low level of expression of *MAFB* found in nearly all mammalian tissues has functionally important consequences for antiviral responses. There is ample support for the view that cells, even in the absence of virus infection, are constitutively exposed to low-level activation signals capable of initiating Type I IFN production, as evidenced by the low-level constitutive phosphorylation observed for *IRF3* and *IRF7*[20],[21]. Spontaneous induction of Type I IFN should be tightly regulated in uninfected cells since chronic activation diminishes host fitness, facilitates autoimmune disease and induces tissue injury. We propose that as a constitutive inhibitor of the Type I IFN pathway, *MAFB* buffers cells against unwarranted induction of Type I IFN. In uninfected cells, *MAFB* proteins might be localized near the *IFN-α* and *β* promoters or other *IRF3* regulated genes, an affiliation presumably mediated by nearby AP-1 or MARE motifs, and exhibits a weak transcriptional activity. Upon adventitious binding of activated *IRF3* to the promoter, *MAFB* masks *IRF3* from *CBP* by binding to the C-terminal IAD domain of *IRF3*, inhibiting interaction of *IRF3* and *CBP* and thereby preventing the formation of functional pre-initiation complexes. *MAFB* might also bind to *IRF3* in the nucleoplasm, interfering with cofactor-mediated recruitment of *IRF3* to relevant promoters. Upon virus infection, the fluxes of activated *IRF3* to the nucleus and recruitment of *IRF3* to relevant promoters significantly increase. Further, *IRF3* binding to *MAFB* in the nucleoplasm might counteract the *MAFB*-mediated inhibition by reducing the pool size of free *MAFB* as recruitment of *IRF3* to the promoters increases, accelerating the production of Type I IFN, which is further amplified by its positive feedback loop. *MAFB* expression might be downregulated, depending on cell type, to facilitate *IRF3*-dependent transactivation. In this way, *MAFB* could create an inhibitory threshold for active Type I IFN induction, with the exact nature of this threshold be determined by cell-type specific *MAFB* expression and its regulation. The dual role of

MAFB as activator and coactivation inhibitor might be intrinsically linked, co-locating *MAFB* in the chromatin neighborhood of highly sensitive promoters and thereby preventing stochastic fluctuation from provoking runaway amplification.

The mechanism of inhibitory action of *MAFB* is distinct from that of previously described repressors since, unlike *IRF2*[44], *MAFB* directly binds to *IRF3* and *IRF7*, and does not directly inhibit *NF-κB*-dependent transactivation. In addition, unlike *PIN1*[45] that targets *IRF3* for ubiquitination and subsequent proteasome-mediated degradation, *MAFB* coexpression does not reduce *IRF3* protein abundance. The dual mode of action of *MAFB* as activator and coactivation inhibitor is distinguishable from that of glucocorticoid receptor, a well-documented dual-regulator of transcription[46], since the *MAFB* activity does not depend strongly on its direct association with *CBP*.

In addition to its effects on *IRF3*, *MAFB* might also exert inhibitory influences on *IRF7*-dependent transcriptional activation under physiological conditions. For example, in cell types with high constitutive *IRF7* expression, such as plasmacytoid dendritic cells and macrophages, cells should also restrain ectopic induction of *IRF7*-dependent transcription. Our results combined with evidence of elevated expression of *MAFB* in these cells compared to other cell types (http://biogps.gnf.org), suggest that *MAFB* might also be important in this process. However, the mode of action of *MAFB* on *IRF7* might differ to that observed for *IRF3* since virus infection induces significant recruitment of *CBP* to *IRF3*, but not *IRF7*[18–21], and efficient binding of *MAFB* to *IRF7* requires the DNA binding domain of *IRF7*, raising the possibility that *MAFB* interferes with *IRF7* DNA binding. Further, our mathematical model suggests that in cell types with elevated expression of *MAFB*, regulation of recruitment and binding of an interferon-inducing transcription factor to a relevant promoter might constitute a primary mode of action of *MAFB* for controlling the *IFN-β* activation (Supplementary Information), supporting the view that *MAFB* functions as a constitutive inhibitor of *IRF7*-dependent transactivation in these cells. We also found that, unlike *TBK1*, *MAFB* showed significant binding to *IKKε*, which, combined with its inhibitory effect on *IRF7*, raises the possibility that *MAFB* also functions to inhibit late phase interferon signaling.

Regulation of *MAFB* expression in response to pathogen triggers, combined with the unstable nature of *MAFB* protein[47], its weak transforming activity[47] and its ability to strongly repress Type I IFN induction, might enable host cells to respond rapidly to viral pathogens. *MAFB* exhibits a myeloid expression pattern with prominent transcription in monocytes and macrophages[5,6], implying that it broadly shapes the innate immune potential of the organism toward an antibacterial (i.e. monocytic or macrophage) instead of an antiviral (dendritic cell) capability. Because *MAFA* is highly expressed in mature β cells and might play a fundamental role in regulating survival and function of these cells[7,8], *MAFB* might be dispensable or at least not central for islet function and hence therapeutic inhibition of *MAFB* with the intent of clearing islet infection might not have adverse consequences for glucose homeostasis. Collectively, our results raise the possibility that *MAFB* expression and regulation has important consequences for Type I IFN responses and predicts a lineage dependence of viral susceptibility that could have important consequences for diseases of viral or autoimmune etiology.

Methods

Plasmids and mutagenesis

Human and mouse expression plasmids were from Open Biosystems (Huntsville, AL) or OriGene (Rockville, MD) unless otherwise specified. Full-length or truncated open reading frames from plasmids were subcloned into pCMV-HA (Clontech), which was modified to remove the HA-tag, or to add an N- or C-terminal Flag-tag. The *IRF3* nuclear localization sequence, amino acids 71 to 89, was added to the N-terminal end of the C-terminal *IRF3* and *IRF7* deletion mutants (*IRF3*(134-427), *IRF3*(197-427), *IRF7*(151-503) and *IRF7*(305-503)). Constitutively active *IRF3*[18] and DNA binding- and sumoylation-deficient mutants of *MAFB*[23],[26] were generated by site-directed mutagenesis PCR. For *in vitro* translation, N-terminal His-tagged *MAFB* was subcloned into the pET-28 vector (EMD Biosciences). Gal4-*IRF3* fusion plasmids were constructed using the pM vector (Clontech). Transcriptional reporters were generated as summarized in Supplementary Table 1.

Cell culture, transfection and luciferase assay

Cell lines were cultured in DMEM, and MEFs lacking *Mafb* were cultured in IMDM. Both media were supplemented with 10% calf serum plus iron and 15 μg/ml gentamycin, and further with 50 μM β-mercaptoethanol for IMDM. 293ETN and HEC1B cells were transfected using TransFectin (BioRad). HeLa, HT-1080, MIN6 and RAW 264.7 cells were transfected using Lipofectamine LTX (Invitrogen). MEFs lacking *Mafb* were transfected using the Amaxa nucleofection system (LONZA). For luciferase assays, cell lines were plated in either 96- or 48-well plates at 4×10^4 cells per well. Unless otherwise specified, cells were transfected with 100 ng of an expression or empty control plasmid together with 10 ng of a luciferase reporter, and 10 ng of pRL-TK Renilla (Promega). For MEFs lacking *Mafb*, 10^6 cells were transfected with 2–3 μg of an expression plasmid and 500 ng of a luciferase reporter, and then transfected cells were plated on 48-well plates at 4×10^4 cells per well. For stimulation, 25 μg/ml of poly(I:C) (GE Healthcare), 50 ng/ml of TNFα (R&D Systems) or 60 ng/ml of PMA (Sigma) were added to media at 24 h post-transfection. *RIG-I(N)*, *MDA5(N)* or *MyD88* expression plasmid (100 ng each) was transfected at 0 h. Cells were infected with NDV (LaSota strain, Charles River Laboratories) or VSV-Luc (luciferase-inserted Indiana strain of VSV[48]) at the indicated hemagglutination (HA) units or multiplicity of infection (MOI) 24 h post-transfection. At various times after transfection, *Photinus* luciferase activity in total cell lysates was measured using Steady-Lite HTS luciferase substrate (Perkin Elmer), or both *Photinus* and *Renilla* luciferase activities were measured using the Dual Luciferase Assay System (Promega).

RNA interference

Lentiviral shRNA vector and pre-designed siRNAs for knockdown of human *MAFB* were purchased from Sigma (shRNA (TRCN0000017681)), Ambion (α-MAFB-1 (s19279), α-MAFB-2 (s19280) and α-MAFB-3 (a pool of s19279 and s19280)) and Dharmacon (α-MAFB-4 (L-009018)). Empty pLKO.1puro vector or non-targeting siRNAs from the corresponding manufacturers were used as controls. For luciferase assays, cells were transfected with either 100 ng of the shRNA or 5 pmol of a siRNA together with luciferase reporter.

Real-time PCR and ELISA

Total RNA was isolated from cells using the RNeasy RNA extraction kit (Qiagen), and cDNA was prepared using the iScript cDNA Synthesis Kit (Bio-Rad). Real-time PCR was performed using an iQ5 RT-PCR Detection System (Bio-Rad) and iQ SYBR Green Supermix (Bio-Rad). Primers are summarized in Supplementary Table 2. Secreted *Ifn-β* protein in cell supernatants was measured using murine *Ifn-β* ELISA Kit (PBL Biomedical).

Immunoblotting

For immunoprecipitation, cell lysates were incubated either with Anti-Flag M2 or Anti-HA Affinity Gel (Sigma), or with an appropriate antibody (anti-*CBP* (sc-369), Santa Cruz; anti-*MAFB* (MAB3810), R&D Systems), followed by protein A/G agarose (Sigma). Immunoblotting used the following antibodies: anti-*IRF3* (sc-9082, Santa Cruz), anti-HA (MMS-101P, Covance), anti-β-actin (ab8226, Abcam), Goat anti-mouse and anti-Rabbit IRDye 800CW (LI-COR) and IRDye800 anti-Flag and anti-HA (Rockland). Immunocomplexes were visualized using an Odyssey Infrared Imaging System (LI-COR).

EMSA and chromatin immunoprecipitation

Electrophoretic mobility shift assays were based on methods described previously[19,20]. Flag-tagged *IRF3* and *MAFB* were purified using M2 Affinity Gel. *In vitro* translated His-*MAFB* was produced using the TNT Coupled Reticulocyte Lysate System (Promega). All nuclear extracts were treated with 1% deoxycholate to reduce *CBP* effects on *IRF3* DNA binding. Supershift assays were performed using Anti-Flag M2 (Sigma) and anti-His (A00186, GenScript) antibodies. Probes used in the study are summarized in Supplementary Table 3. Chromatin immunoprecipitation was performed according to the manufacturer's recommendations (Magna ChIP A kit, MILLIPORE). Immunoprecipitation was performed using an appropriate antibody (described earlier) and Protein A Magnetic Beads (MILLIPORE). Purified DNA samples were quantified by real-time PCR using the following primers: 5′-tgacataggaaaactgaaagggag (forward) and 5′-gtcctttctccatgggtatgg (backward).

Native PAGE and caspase 3 assay

Native PAGE was performed as described[49]. Caspase 3 activity was measured using the Caspase-Glo 3/7 Assay kit (Promega).

NOD mice and islet isolation

Female NOD/ShiLtJ mice were obtained from The Jackson Laboratory. Mice were maintained under SPF conditions in accordance with US Government and local institutional guidelines. Glucose levels were measured weekly using blood samples collected from tail veins. Test groups of mice were sacrificed within 24 hours of glucose measurement. Whole islets were isolated from mice as previously described[43].

Laser capture microdissection

Whole mouse pancreatic tissue was harvested and frozen immediately in OCT® (Sigma). 8 micron cryo-sections were mounted on microscopy slides. Each tissue section was lightly

fixed in 70% ethanol, rinsed with RNAse free diH_2O, and incubated in a toluidine blue solution for 1 min. The stained sections were then dehydrated in increasingly concentrated ethanol 70–100% into xylene. The central core of islets was microdissected and captured onto Arcturus Macro Cap using Veritas Microdissection System (Molecular Devices). The collecting cap was incubated at 42°C for 30 minutes in Arcturus GITC-containing extraction buffer, and RNA was isolated using the Arcturus picopure RNA isolation system (Molecular Devices).

Microarray analysis, mathematical modeling and statistics

Microarray datasets were obtained either from the GEO database (http://www.ncbi.nlm.nih.gov/geo) or directly from the literature, and processed using R. Expression profiles were summarized using the GCRMA method without log2 transformation as implemented in Bioconductor (http://www.bioconductor.org). Expression values were further standardized (to Z-values) for each probe set. Mathematical modeling (Supplementary Information) was performed following a similar approach to ref [50]. Two-tailed Student's t-test or one-way analysis of variance (ANOVA) was applied to compare two or more than two data sets, respectively, using a significance level of 0.05.

Supplementary Material

Refer to Web version on PubMed Central for supplementary material.

Acknowledgments

We thank John Darga for assistance with automated assays and high throughput screens, and Rasma Niedra, Naifang Lu and Weihua Zhou for experimental help. We appreciate the contributions of the Seed and Xavier groups in sharing reagents and information. We are grateful to Satoru Takahashi, Michito Hamada and Doug Engel for KO *Mafb* MEFs and discussion, Sean Whelan for VSV-Luc, Takashi Fujita for the *CBP* construct and Jun-ichi Miyazaki and Donald F Steiner for MIN6 cells. We thank Charles Vanderburg for assistance with LCM. We also thank Marc Wathelet, Rongtuan Lin, Sunmi Han and Horim Lee for helpful discussions.

References

1. Kawai T, Akira S. The role of pattern-recognition receptors in innate immunity: update on Toll-like receptors. Nat Immunol. 2010; 11:373–384. [PubMed: 20404851]
2. Yoneyama M, Fujita T. RNA recognition and signal transduction by RIG-I-like receptors. Immunol Rev. 2009; 227:54–65. [PubMed: 19120475]
3. Motohashi H, O'Connor T, Katsuoka F, Engel JD, Yamamoto M. Integration and diversity of the regulatory network composed of Maf and CNC families of transcription factors. Gene. 2002; 294:1–12. [PubMed: 12234662]
4. Eychene A, Rocques N, Pouponnot C. A new MAFia in cancer. Nat Rev Cancer. 2008
5. Wang PW, et al. Human KRML (MAFB): cDNA cloning, genomic structure, and evaluation as a candidate tumor suppressor gene in myeloid leukemias. Genomics. 1999; 59:275–281. [PubMed: 10444328]
6. Kelly LM, Englmeier U, Lafon I, Sieweke MH, Graf T. MafB is an inducer of monocytic differentiation. Embo J. 2000; 19:1987–1997. [PubMed: 10790365]
7. Artner I, et al. MafB: an activator of the glucagon gene expressed in developing islet alpha- and beta-cells. Diabetes. 2006; 55:297–304. [PubMed: 16443760]
8. Nishimura W, et al. A switch from MafB to MafA expression accompanies differentiation to pancreatic beta-cells. Dev Biol. 2006; 293:526–539. [PubMed: 16580660]

9. Yoneyama M, et al. The RNA helicase RIG-I has an essential function in double-stranded RNA-induced innate antiviral responses. Nat Immunol. 2004; 5:730–737. [PubMed: 15208624]
10. Kato H, et al. Differential roles of MDA5 and RIG-I helicases in the recognition of RNA viruses. Nature. 2006; 441:101–105. [PubMed: 16625202]
11. Maniatis T, et al. Structure and function of the interferon-beta enhanceosome. Cold Spring Harb Symp Quant Biol. 1998; 63:609–620. [PubMed: 10384326]
12. Escalante CR, Nistal-Villan E, Shen L, Garcia-Sastre A, Aggarwal AK. Structure of IRF-3 bound to the PRDIII-I regulatory element of the human interferon-beta enhancer. Mol Cell. 2007; 26:703–716. [PubMed: 17560375]
13. Moriguchi T, et al. MafB is essential for renal development and F4/80 expression in macrophages. Mol Cell Biol. 2006; 26:5715–5727. [PubMed: 16847325]
14. Fitzgerald KA, et al. IKKepsilon and TBK1 are essential components of the IRF3 signaling pathway. Nat Immunol. 2003; 4:491–496. [PubMed: 12692549]
15. Sharma S, et al. Triggering the interferon antiviral response through an IKK-related pathway. Science. 2003; 300:1148–1151. [PubMed: 12702806]
16. Hiscott J. Triggering the innate antiviral response through IRF-3 activation. J Biol Chem. 2007; 282:15325–15329. [PubMed: 17395583]
17. Tamura T, Yanai H, Savitsky D, Taniguchi T. The IRF family transcription factors in immunity and oncogenesis. Annu Rev Immunol. 2008; 26:535–584. [PubMed: 18303999]
18. Lin R, Heylbroeck C, Pitha PM, Hiscott J. Virus-dependent phosphorylation of the IRF-3 transcription factor regulates nuclear translocation, transactivation potential, and proteasome-mediated degradation. Mol Cell Biol. 1998; 18:2986–2996. [PubMed: 9566918]
19. Lin R, Genin P, Mamane Y, Hiscott J. Selective DNA binding and association with the CREB binding protein coactivator contribute to differential activation of alpha/beta interferon genes by interferon regulatory factors 3 and 7. Mol Cell Biol. 2000; 20:6342–6353. [PubMed: 10938111]
20. Wathelet MG, et al. Virus infection induces the assembly of coordinately activated transcription factors on the IFN-beta enhancer in vivo. Mol Cell. 1998; 1:507–518. [PubMed: 9660935]
21. Yoneyama M, et al. Direct triggering of the type I interferon system by virus infection: activation of a transcription factor complex containing IRF-3 and CBP/p300. Embo J. 1998; 17:1087–1095. [PubMed: 9463386]
22. Kumar KP, McBride KM, Weaver BK, Dingwall C, Reich NC. Regulated nuclear-cytoplasmic localization of interferon regulatory factor 3, a subunit of double-stranded RNA-activated factor 1. Mol Cell Biol. 2000; 20:4159–4168. [PubMed: 10805757]
23. Cordes SP, Barsh GS. The mouse segmentation gene kr encodes a novel basic domain-leucine zipper transcription factor. Cell. 1994; 79:1025–1034. [PubMed: 8001130]
24. Sieweke MH, Tekotte H, Frampton J, Graf T. MafB is an interaction partner and repressor of Ets-1 that inhibits erythroid differentiation. Cell. 1996; 85:49–60. [PubMed: 8620536]
25. Mizukami J, Taniguchi T. The antidiabetic agent thiazolidinedione stimulates the interaction between PPAR gamma and CBP. Biochem Biophys Res Commun. 1997; 240:61–64. [PubMed: 9367882]
26. Tillmanns S, et al. SUMO modification regulates MafB-driven macrophage differentiation by enabling Myb-dependent transcriptional repression. Mol Cell Biol. 2007; 27:5554–5564. [PubMed: 17548468]
27. Napolitani G, Rinaldi A, Bertoni F, Sallusto F, Lanzavecchia A. Selected Toll-like receptor agonist combinations synergistically trigger a T helper type 1-polarizing program in dendritic cells. Nat Immunol. 2005; 6:769–776. [PubMed: 15995707]
28. Stetson DB, Medzhitov R. Recognition of cytosolic DNA activates an IRF3-dependent innate immune response. Immunity. 2006; 24:93–103. [PubMed: 16413926]
29. Pruett SB, Schwab C, Zheng Q, Fan R. Suppression of innate immunity by acute ethanol administration: a global perspective and a new mechanism beginning with inhibition of signaling through TLR3. J Immunol. 2004; 173:2715–2724. [PubMed: 15294990]
30. Hammer M, et al. Dual specificity phosphatase 1 (DUSP1) regulates a subset of LPS-induced genes and protects mice from lethal endotoxin shock. J Exp Med. 2006; 203:15–20. [PubMed: 16380512]

31. Cao W, et al. Toll-like receptor-mediated induction of type I interferon in plasmacytoid dendritic cells requires the rapamycin-sensitive PI(3)K-mTOR-p70S6K pathway. Nat Immunol. 2008; 9:1157–1164. [PubMed: 18758466]
32. Ylipaasto P, et al. Global profiling of coxsackievirus- and cytokine-induced gene expression in human pancreatic islets. Diabetologia. 2005; 48:1510–1522. [PubMed: 15991020]
33. Gaither LA, et al. Multiple cyclophilins involved in different cellular pathways mediate HCV replication. Virology. 2010; 397:43–55. [PubMed: 19932913]
34. Hyoty H, Taylor KW. The role of viruses in human diabetes. Diabetologia. 2002; 45:1353–1361. [PubMed: 12378375]
35. Ylipaasto P, et al. Enterovirus infection in human pancreatic islet cells, islet tropism in vivo and receptor involvement in cultured islet beta cells. Diabetologia. 2004; 47:225–239. [PubMed: 14727023]
36. Foulis AK, et al. A search for the presence of the enteroviral capsid protein VP1 in pancreases of patients with type 1 (insulin-dependent) diabetes and pancreases and hearts of infants who died of coxsackieviral myocarditis. Diabetologia. 1990; 33:290–298. [PubMed: 2376300]
37. Maffei A, et al. Identification of tissue-restricted transcripts in human islets. Endocrinology. 2004; 145:4513–4521. [PubMed: 15231694]
38. Marselli L, et al. Gene expression of purified beta-cell tissue obtained from human pancreas with laser capture microdissection. J Clin Endocrinol Metab. 2008; 93:1046–1053. [PubMed: 18073315]
39. See DM, Tilles JG. Pathogenesis of virus-induced diabetes in mice. J Infect Dis. 1995; 171:1131–1138. [PubMed: 7751687]
40. Chehadeh W, et al. Persistent infection of human pancreatic islets by coxsackievirus B is associated with alpha interferon synthesis in beta cells. J Virol. 2000; 74:10153–10164. [PubMed: 11024144]
41. Serreze DV, Prochazka M, Reifsnyder PC, Bridgett MM, Leiter EH. Use of recombinant congenic and congenic strains of NOD mice to identify a new insulin-dependent diabetes resistance gene. J Exp Med. 1994; 180:1553–1558. [PubMed: 7931087]
42. Drescher KM, Kono K, Bopegamage S, Carson SD, Tracy S. Coxsackievirus B3 infection and type 1 diabetes development in NOD mice: insulitis determines susceptibility of pancreatic islets to virus infection. Virology. 2004; 329:381–394. [PubMed: 15518817]
43. Carter JD, Dula SB, Corbin KL, Wu R, Nunemaker CS. A Practical Guide to Rodent Islet Isolation and Assessment. Biol Proced Online. 2009
44. Senger K, et al. Gene repression by coactivator repulsion. Mol Cell. 2000; 6:931–937. [PubMed: 11090630]
45. Saitoh T, et al. Negative regulation of interferon-regulatory factor 3-dependent innate antiviral response by the prolyl isomerase Pin1. Nat Immunol. 2006; 7:598–605. [PubMed: 16699525]
46. Revollo JR, Cidlowski JA. Mechanisms generating diversity in glucocorticoid receptor signaling. Ann N Y Acad Sci. 2009; 1179:167–178. [PubMed: 19906239]
47. Pouponnot C, et al. Cell context reveals a dual role for Maf in oncogenesis. Oncogene. 2006; 25:1299–1310. [PubMed: 16247450]
48. Whelan SP, Ball LA, Barr JN, Wertz GT. Efficient recovery of infectious vesicular stomatitis virus entirely from cDNA clones. Proc Natl Acad Sci U S A. 1995; 92:8388–8392. [PubMed: 7667300]
49. Iwamura T, et al. Induction of IRF-3/-7 kinase and NF-kappaB in response to double-stranded RNA and virus infection: common and unique pathways. Genes Cells. 2001; 6:375–388. [PubMed: 11318879]
50. Kim H, Perelson AS. Viral and latent reservoir persistence in HIV-1-infected patients on therapy. PLoS Comput Biol. 2006; 2:e135. [PubMed: 17040122]

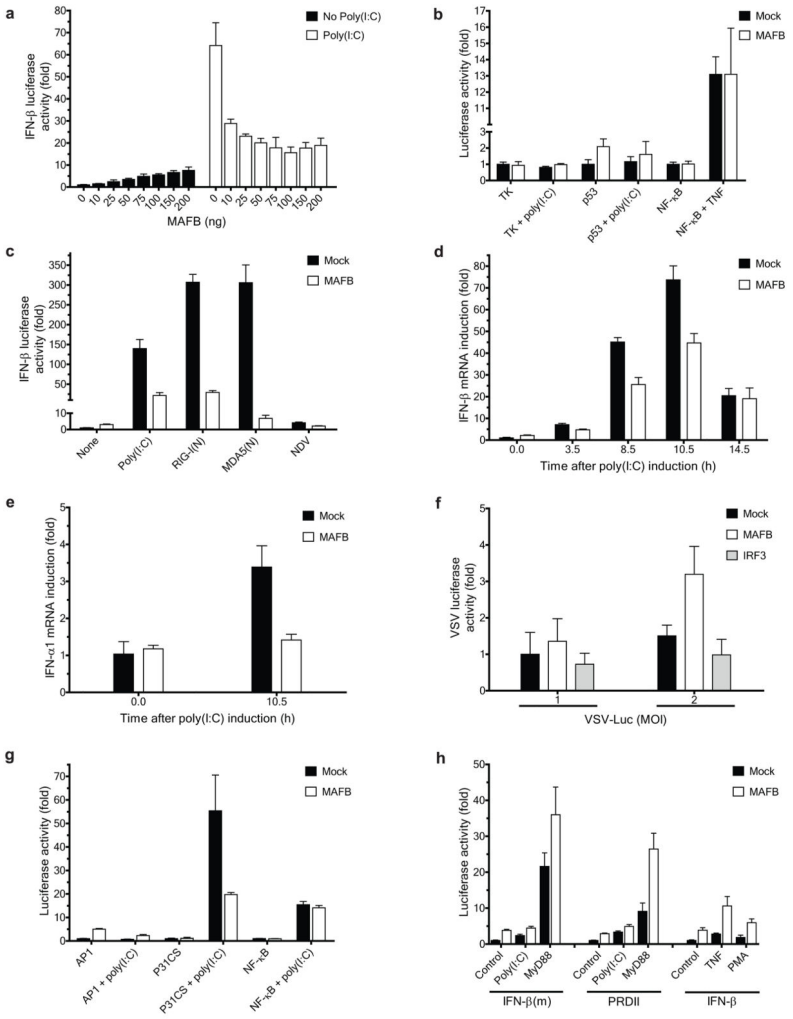

Figure 1.

MAFB negatively regulates Type I Interferon induction. (**a–c, g, h**) Effect of *MAFB* on viral elicitor-mediated activation of luciferase reporters: (**a, c**) IFN-β-Luc, (**b**) TK Renilla, p53-Luc, or NF-κB-Luc, (**g**) AP1-Luc, P31CS-Luc, or NF-κB-Luc, and (**h**) IFN-β(m)-Luc (an *IRF3* binding deficient mutant of *IFN-β*), PRDII-Luc (a PRDI, III and IV-deleted mutant of *IFN-β*), or IFN-β-Luc (10 ng each). Poly(I:C) (25 μg/ml), TNF-α (50 ng/ml), NDV (12 HA units), or PMA (60 ng/ml) was added at 24 h post-transfection. *RIG-I(N)*, *MDA5(N)* or *MyD88* (100 ng each) was transfected at 0 h. Luciferase activity was measured at 48 h (poly(I:C), TNF and PMA) or 32 h (NDV, *RIG-I(N)*, *MDA5(N)* and *MyD88*) post-transfection, and is displayed as fold increase relative to the basal level luciferase activity in mock-transfected control without stimulation for each reporter. (**d, e**) Effect of *MAFB* on activation of endogenous (**d**) *IFN-β* and (**e**) *IFN-α1* promoters. mRNA levels were measured by RT-PCR at the times depicted after poly(I:C) induction. All values were normalized to β-actin, and the values of each gene were further normalized to those before induction. (**f**) Effect of *MAFB* on VSV replication. Cells were infected with VSV-Luc at indicated MOIs 24 h after transfection with an indicated vector (25 ng each). VSV replication was assayed by measuring luciferase activity at 9 h post-infection. Data indicate mean ± SD of at least

three (**d**, **e**) or four (**a–c, f–h**) within-plate replicates, and results representative of two (**b**, **h**) or three (**a**, **c–g**) independent experiments are shown. 293ETN cells were used in all panels.

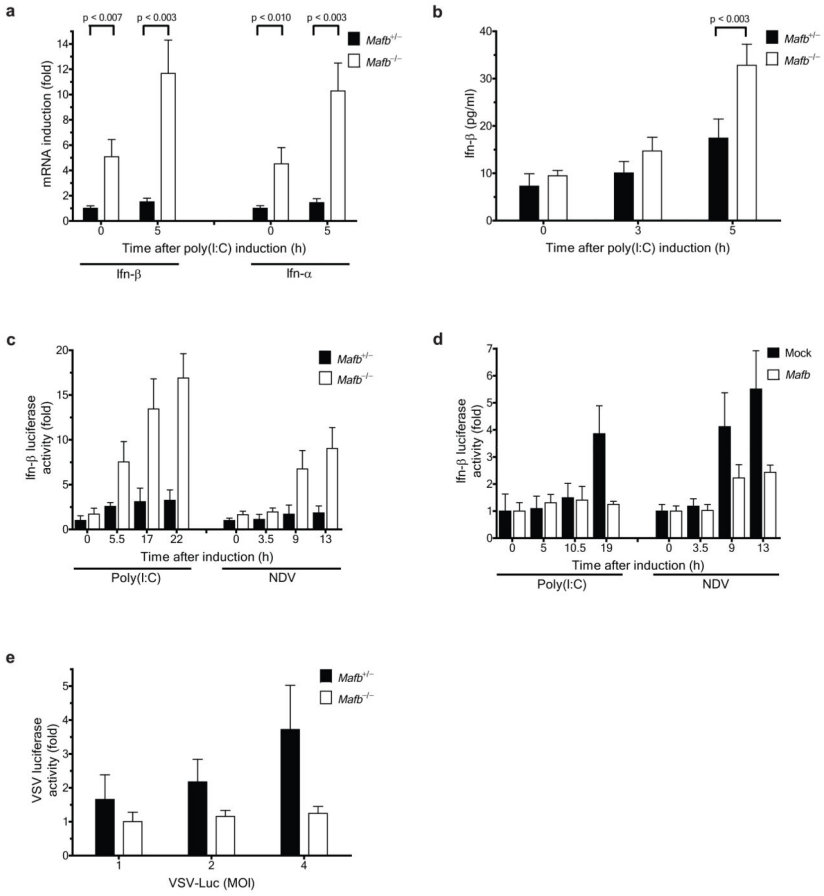

Figure 2.

Knockout of *Mafb* facilitates Type I interferon induction. (**a**, **b**) Comparison of activation of endogenous *Ifn-α* and *Ifn-β* promoters between $Mafb^{-/-}$ and $Mafb^{+/-}$ MEFs by (**a**) RT-PCR and (**b**) ELISA. (**a**) The mRNA levels and (**b**) secreted *Ifn-β* protein in cell supernatants were measured at the times depicted after poly(I:C) induction. (**a**) All values were normalized to β-actin, and the values of each gene were further normalized to the corresponding gene value from $Mafb^{+/-}$ MEFs at 0 h. (**c**) $Mafb^{-/-}$ and $Mafb^{+/-}$ MEFs were transfected with a mouse *Ifn-β* luciferase reporter (mIFN-β-Luc). (**d**) $Mafb^{-/-}$ MEFs were transfected with vector control or mouse *Mafb* together with mIFN-β-Luc. (**c**, **d**), poly(I:C) or NDV (6 HA units) was added at 24 h post-transfection, and luciferase activity was measured at the indicated times after stimulation as fold increase relative to the basal level luciferase activity in $Mafb^{+/-}$ MEFs (**c**) or mock-transfected control (**d**) before stimulation. (**e**) $Mafb^{-/-}$ and $Mafb^{+/-}$ MEFs were infected with VSV-Luc at indicated MOIs. Luciferase activity was measured at 9 h post-infection, and is displayed as fold increase relative to the activity in $Mafb^{-/-}$ MEFs at MOI = 1. Data indicate mean ± SD of at least three (**a**) or four (**b**–**e**) within-plate replicates, and results representative of three independent experiments are shown.

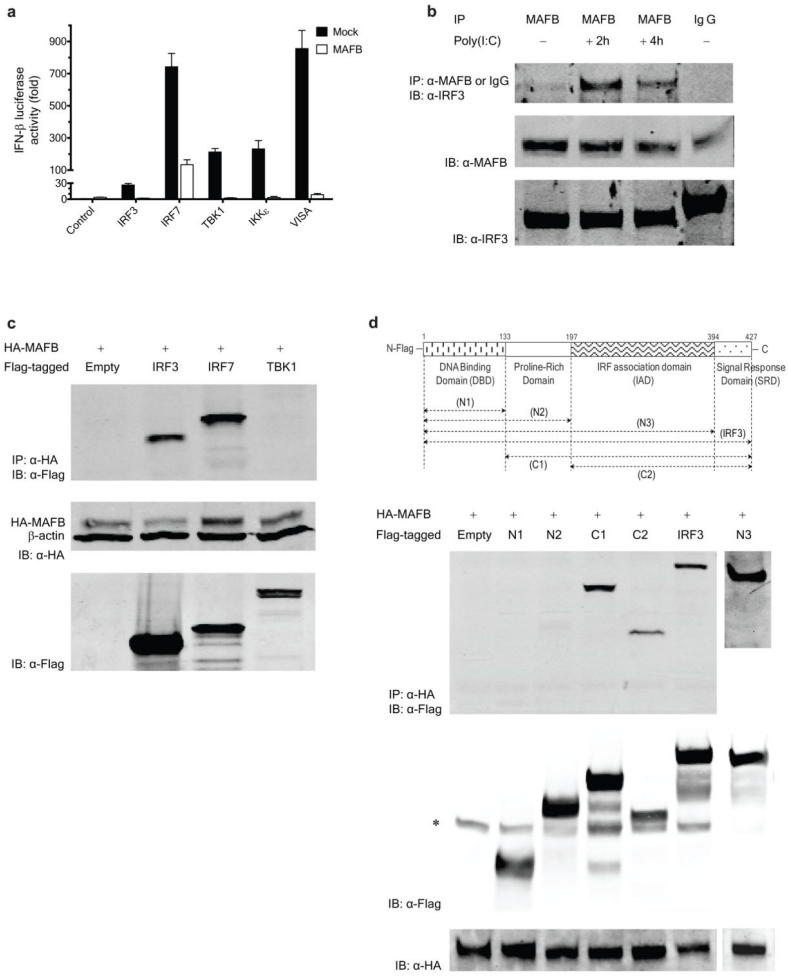

Figure 3.

MAFB interferes with *IRF3* and *IRF7* activities. (**a**) 293ETN cells were transfected with IFN-β-Luc and an expression vector encoding the proteins shown (100 ng each) together with empty control or *MAFB* (100 ng each). Luciferase activity was measured at 48 h post-transfection (at least in quadruple) as fold increase relative to the basal level luciferase activity in mock-transfected control without *MAFB* expression. (**b**) Interaction of endogenous *MAFB* with endogenous *IRF3* in HeLa cells at the indicated times after poly(I:C) stimulation. IP and IB denote immunoprecipitation and immunoblotting, respectively. (**c**) Interaction of HA-*MAFB* with Flag-tagged proteins in 293ETN cells (upper panel). At 48 h after transfection, whole cell extracts were immunoprecipitated with anti-HA antibody and then immunoblotted for *IRF3*, *IRF7* and *TBK1* with anti-Flag antibody. (**d**) Interaction of HA-*MAFB* with Flag-tagged *IRF3* deletion mutants in 293 ETN cells. A schematic diagram of full-length *IRF3* and its deletion mutants is shown at the top. The bands indicated by * denote nonspecific bands. Immunoblot using 6% (**b**) or 3% (**c, d**) of input lysate are also shown. All cell extracts were run on 10% SDS-PAGE.

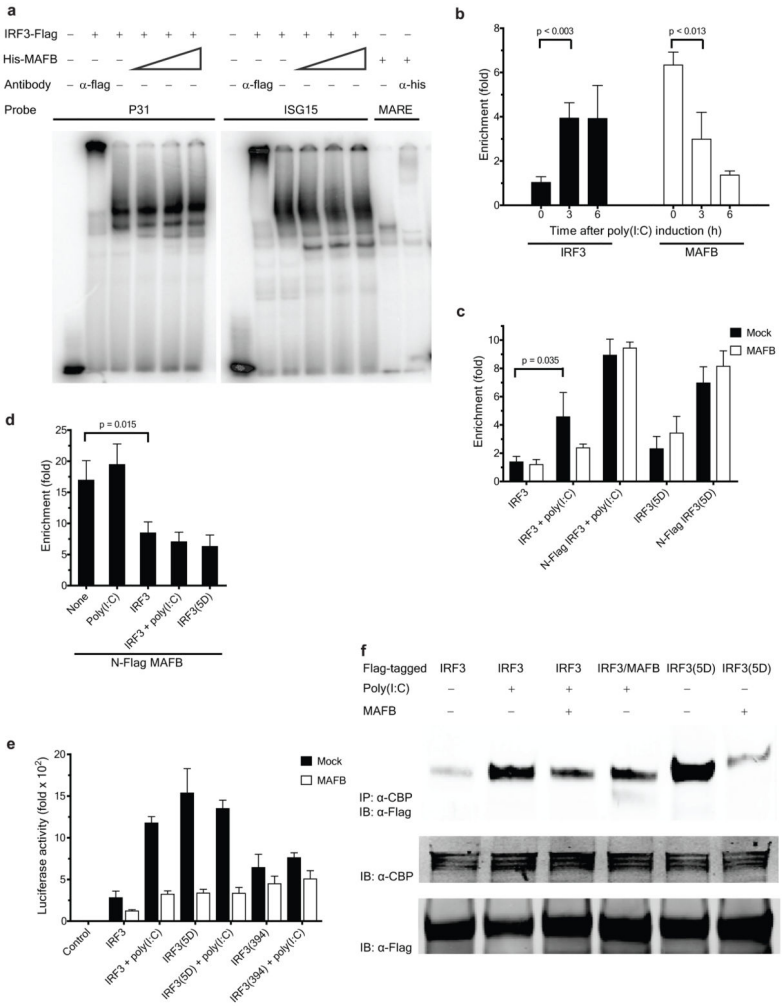

Figure 4.

Mechanisms underlying *MAFB*-mediated suppression of Type I IFN induction. (**a**) EMSA analysis using immunopurified *IRF3*. C-terminal Flag-*IRF3* Protein (0.6 μg) was incubated with a ^{32}P-labeled PRDIII-PRDI (P31) or ISG15 probe in the absence and presence of *in vitro* translated N-terminal His-*MAFB* (1, 3 and 5 μl for lanes 4(10), 5(11) and 6(12), respectively). Binding activity and specificity of Flag-*IRF3* and His-*MAFB* (1μl) to indicated probes were demonstrated by supershift experiments. (**b–d**), ChIP assay to determine the recruitment of (**b**) endogenous *IRF3* and *MAFB*, (**c**) overexpressed *IRF3* and (**d**) overexpressed *MAFB* to the *IFN-β* promoter. The fold enrichment of the *IFN-β* promoter over IgG control was quantified using qPCR. (**b**) HeLa cells were cross-linked at the times depicted after poly(I:C) induction. (**c, d**), 293ETN cells were transfected with depicted forms of *IRF3* and *MAFB* vectors. All samples were cross-linked at 36 h post-transfection. (**e**) Effect of *MAFB* on activation of $(Gal4)_5$-Luc by fusion proteins of the Gal4 DBD and *IRF3* variants. 293ETN cells were transfected with $(Gal4)_5$-Luc and Gal4-*IRF3* vectors together with empty control or *MAFB*. Luciferase activity was measured at 48 h post-transfection. (**f**) Effect of *MAFB* on the interaction of *IRF3* with *CBP*. 293ETN cells were transfected with indicated Flag-tagged vectors. Where indicated, untagged *MAFB* was

cotransfected at 0 h. Cell lysates were prepared at 36 h post-transfection. (**c–f**), poly(I:C) was added at 24 h post-transfection as indicated.

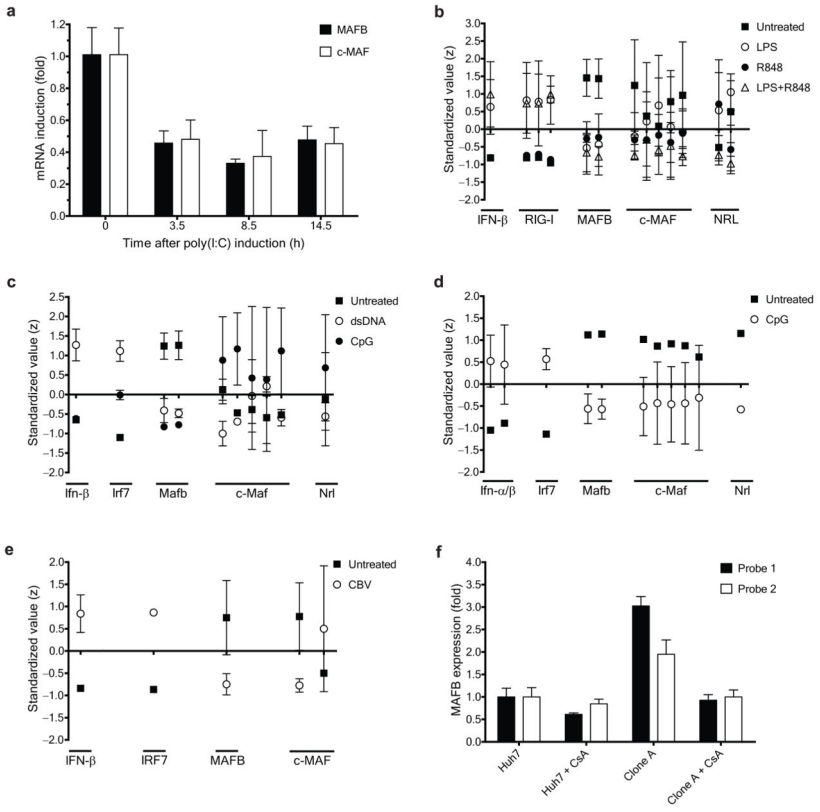

Figure 5.

Regulation of *MAFB* expression in response to pathogen triggers. (**a**) The levels of *MAFB* and *c-MAF* mRNAs in 293ETN cells were measured by RT-PCR at the indicated times after poly(I:C) induction. Values were normalized to β-actin expression, and further normalized to the corresponding value before poly(I:C) induction. (**b–e**), Regulatory patterns of expression of *MAFB* and other large MAF transcription factors in response to pathogen-mimetic stimulation in a variety of cell types. (**b**) Human monocyte-derived dendritic cells in response to LPS or the synthetic imidazoquinoline resiquimod R848[27], a TLR7/8 agonist, (**c**) murine bone marrow-derived dendritic cells in response to lipid-transfected double-stranded DNA (dsDNA) or CpG oligonucleotides[28], a TLR9 agonist, (**d**) murine plasmacytoid dendritic cells (pDC) in response to CpG oligonucleotides[31], and (**e**) human pancreatic islet cells in response to coxsackievirus[32]. Microarray expression values were standardized (to Z-values) for each probe set separately, and data are expressed as mean ± SD of each treatment for each indicated probe (x-axis). (**f**) Expression patterns of *MAFB* in naïve and HCV-replicon-containing (Clone A) Huh7 cells. Microarray expression values (measured in triplicate)[33] were normalized to the values of naïve Huh7.

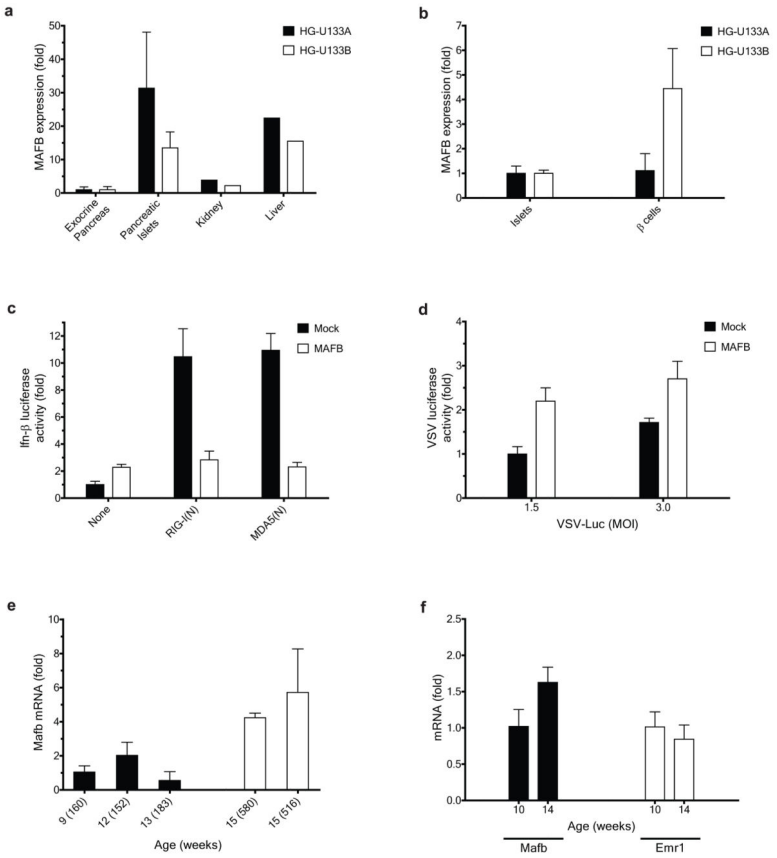

Figure 6.

Roles of *MAFB* in pancreatic β cells. (**a**, **b**). Microarray-based expression patterns of *MAFB* in human pancreatic tissues. (**a**) Islet versus exocrine pancreas[37] and (**b**) Purified β cells versus total islet cells[38]. For each microarray platform, *MAFB* expression values were normalized to the value of (**a**) exocrine pancreas and (**b**) total islet cells. Data indicate (**a**) mean ± SD (for pancreatic tissues) and a single pooled value (for kidney and liver) of at least two donors, and (**b**) mean ± SD of three donors. (**c, d**), Effect of human *MAFB* overexpression on (**c**) mIFN-β-Luc activation and (**d**) VSV replication in a murine β cell line. MIN6 cells transfected with empty control or *MAFB* were (**c**) cotransfected with mIFN-β-Luc together with *RIG-I(N)* or *MDA5(N)* at 0 h or (**d**) infected with VSV-Luc 24 h later. Luciferase activities were measured at 34 h post-transfection. (**e**, **f**) Age-dependent changes in *Mafb* expression in islet tissue of NOD mice. (**e**) beta cell-rich core of islets collected using LCM and (**f**) whole islets isolated by collagenase perfusion. *Mafb* and *Emr1* mRNA levels were measured by RT-PCR at the age indicated. (**e**) The blood glucose level for each mouse (mg/dl) is shown in parenthesis. (**f**) For each age group, two mice were used to obtain pooled total RNA (with blood glucose (mg/dl) of 115 and 143 for 10-week-old and 550 and 579 for 14-week-old). Values were normalized to GAPDH expression, and further normalized to the corresponding values from the youngest mouse (group).